Chapter 8

Power Cylinder System for Internal Combustion Engines

Chao Cheng

Additional information is available at the end of the chapter

http://dx.doi.org/10.5772/intechopen.69762

Abstract

Piston ring pack is one of the most critical components for engine performance, durability, and emission. It has become a decisive factor for engine life. From previous study, a three-dimensional ring model has been developed using finite element method to study the interactions between the ring-cylinder liner and the ring-groove side interfaces. The ring-cylinder and ring-groove side contacts are modeled using finite element method based on penalty method optimization algorithm. Ring deformation, reaction forces at the ring sides and ring face, and the twist angles along the entire ring circumference are obtained from the model. However, the dynamic behavior of the ring is still less understood. In this study, the dynamic response of the ring over an engine cycle is studied for a second compression ring with a non-symmetric cross section.

Keywords: power cylinder system, piston, ring pack, cylinder liner, friction, wear, oil consumption, dynamics, finite element, optimization, internal combustion engines

1. Introduction

The internal combustion engine converts thermal energy of the combustible fuel into mechanical energy that moves the piston and eventually the crankshaft. This energy conversion process occurs within the engine power cylinder system. The power cylinder system comprises the following components: piston, piston rings, cylinder liner, wrist pin, and connecting rod.

The piston is the main component that delivers the mechanical energy through reciprocating motion. And this reciprocating motion is transmitted into rotational motion of the crankshaft to output power through the connecting rod. The connecting rod's small end is connected to the piston through the wrist pin, and the rod's big end is connected to the crankshaft. Combustion occurs above the piston in the combustion chamber, which is sealed by the ring pack, especially the top compression of the ring pack. **Figure 1** shows these major components of the power cylinder system.

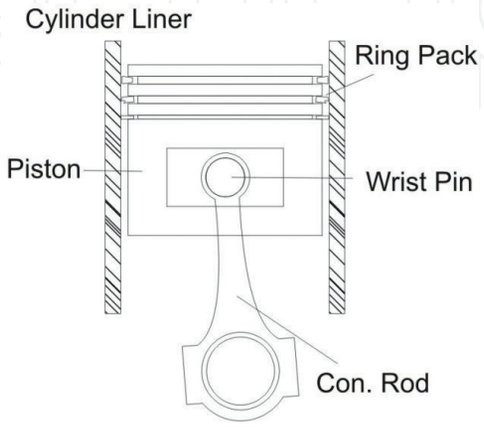

Figure 1. Power cylinder system.

A complete engine cycle consists of four different strokes for a four-stroke engine along with the piston-reciprocating motion. These four strokes are intake stroke, compression stroke, expansion stroke, and exhaust stroke as shown in **Figure 2**.

As for a modern diesel engine, which is known for its better efficiency over its gasoline counterpart, only about 40% of the energy produced by the engine is converted to the engine output

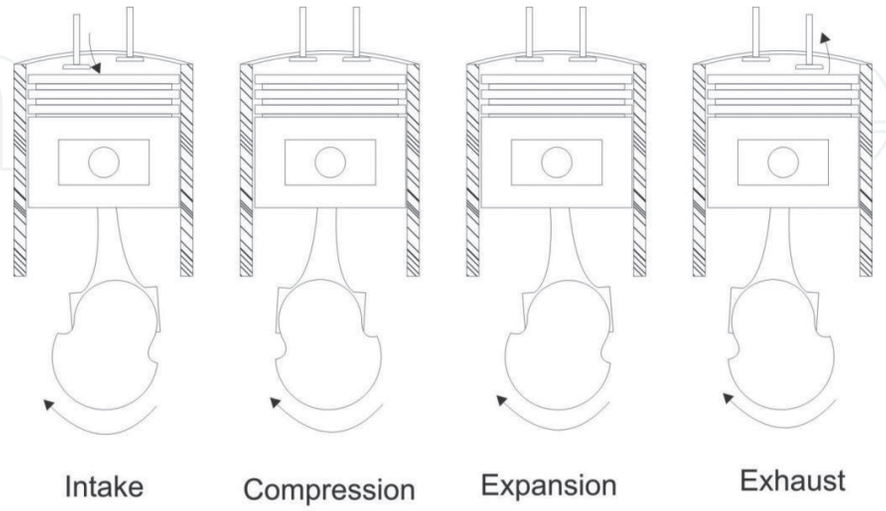

Figure 2. Four strokes for a complete engine cycle.

power. About 4–15% of that energy is wasted as mechanical friction loss. And the rest of the energy, which is almost over half of the chemical energy, is dissipated as other forms, for example, heat transfer, blowby loss, and so on, as shown in **Figure 3** from the study by Richardson [1].

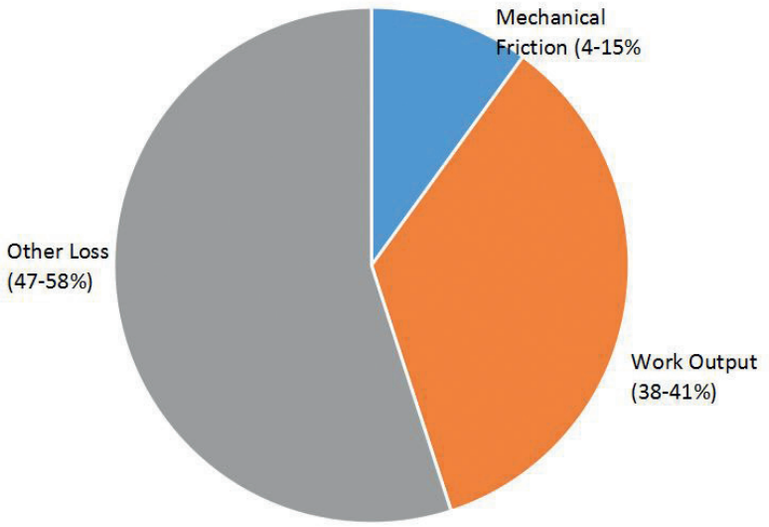

Figure 3. Power distribution for diesel engines.

And about half of the mechanical friction loss is attributed to the friction in the power cylinder system, including the piston, ring pack, and the connecting rod as shown in **Figure 4** [1]. The other part is due to the friction of other components, for example, the valve train system, the crankshaft bearings, and so on.

The friction loss distribution among piston, piston ring pack, and the connecting rod for the power cylinder system can be found in **Figure 5** [1]. As can be found, the piston and ring pack account for higher friction loss than the connecting rod.

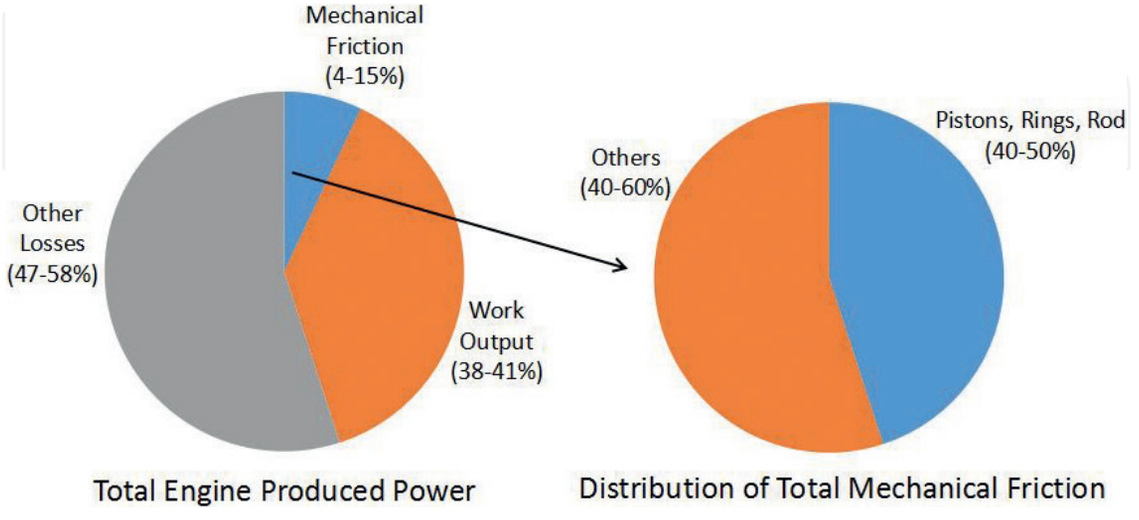

Figure 4. Mechanical friction power distribution.

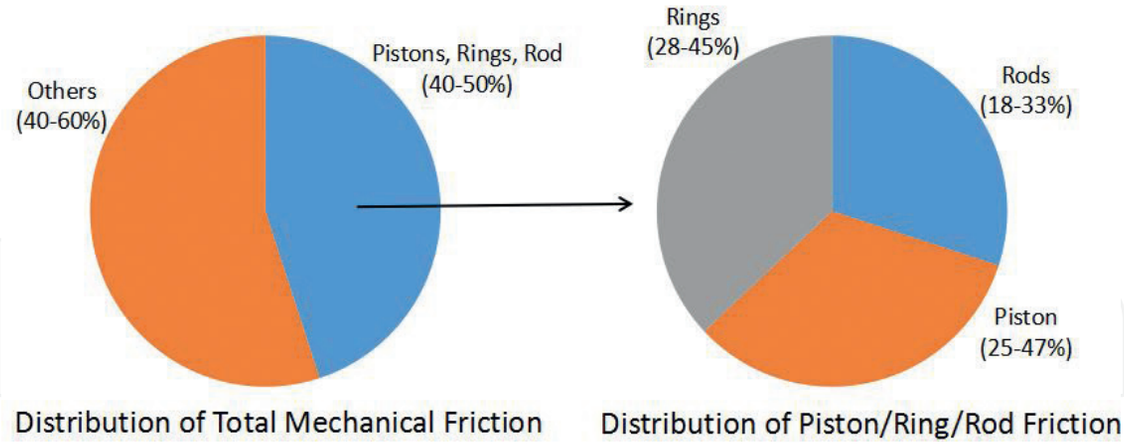

Figure 5. Power cylinder system friction power distribution.

1.1. Piston

The piston of an internal combustion engine is the main component to transmit the thermal energy into mechanical energy. High-pressure gas from the combustion of the fuel-air mixture pushes the piston downward to deliver mechanical energy. Thus, the working condition for the piston is severe. Pistons in small engines are made of aluminum while for large lower speed applications, the pistons are made of cast iron [2]. As the load continues to increase for engines, especially in the heavy-duty industry, steel pistons become widely used nowadays. **Figure 6** shows a typical piston for diesel engine with the definitions of the key geometries shown in **Table 1**.

The piston skirt generally has a barrel/parabolic profile that promotes hydrodynamic lubrication due to the edge effect (**Figure 7**). This skirt profile needs to be optimized in order to minimize piston friction. Piston skirt also grows outward in the radial direction at a high temperature during engine operation.

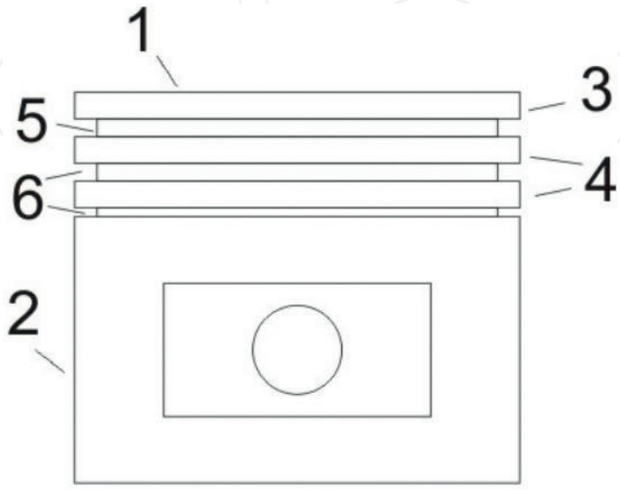

Figure 6. Key piston geometries.

No.	Definitions
1	Piston crown
2	Piston skirt
3	Top land
4	Second and third land
5	Top groove
6	Second and third groove

Table 1. Definitions of key piston geometries.

In addition to the barrel/parabolic profile in the axial direction, piston skirt usually has ovality in the circumference direction as well. The ovality is defined as the difference between the diameter in the thrust axis and the diameter in the pin axis. The ovality is introduced to reduce wear and the risk of scuffing. Development work related to piston dynamics, friction, scuffing, and so on can be found from the references by different researchers [3–11].

1.2. Ring pack

The ring pack is typically composed with three rings: two compression rings and one oil control ring. The main functions of the ring pack are listed as follows:

1. To seal the combustion chamber in conjunction with the piston lands and the cylinder wall, in order to prevent the high-pressure gas from leaking into the crankcase that is wasted in producing power.
2. To control the lubrication oil from getting into the combustion chamber from below the piston as well as to distribute the lubrication oil evenly on the cylinder wall.
3. To transfer heat from the piston to the cylinder wall and eventually to the cooling system. Since the piston crown is exposed to the combustion chamber, it is critical to reduce the piston temperature in order to guarantee the piston's working condition.

Figure 8 shows typical ring packs for modern gasoline and diesel engines.

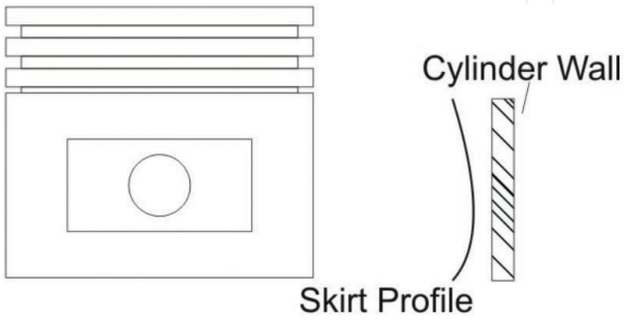

Figure 7. Piston skirt profile.

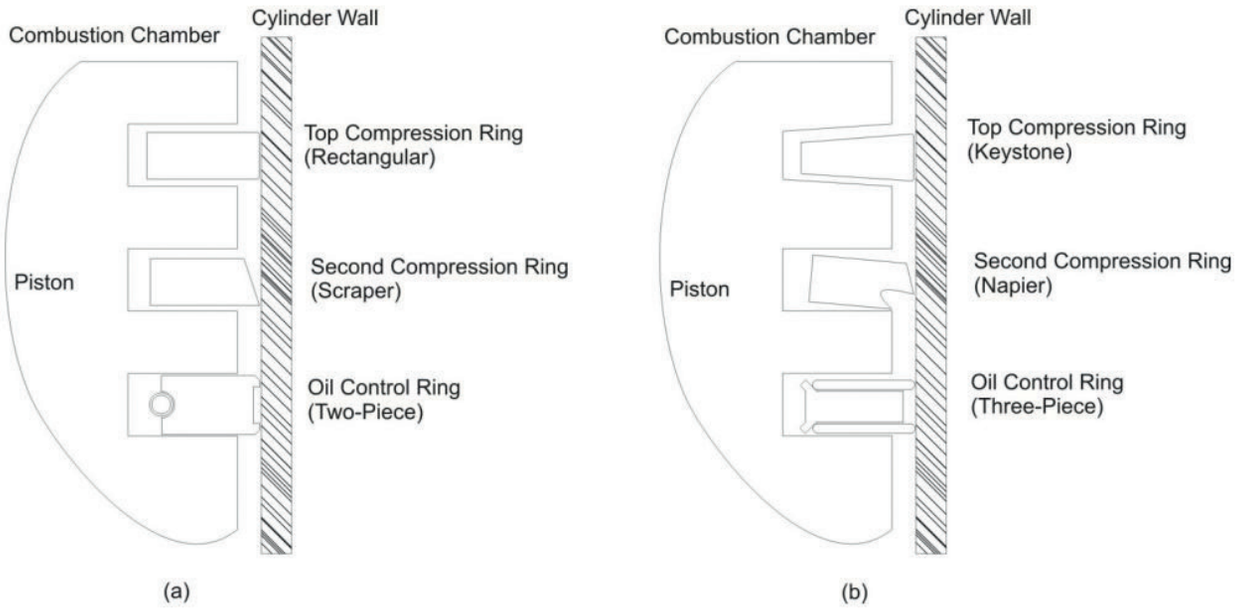

Figure 8. IC engine ring pack: (a) gasoline engine and (b) diesel engine.

1.2.1. Top compression ring

The top compression ring is the first ring and the main component sealing the combustion chamber for engine blowby control. The top ring is also under the most severe working condition since it is directly exposed to the combustion gas and usually under high pressure and high temperature.

The top compression rings for gasoline engine usually have a rectangular cross section. However, for diesel engine operation, the top compression rings usually are keystone rings (**Figure 9**) which promotes the breakup of the deposits between the ring and piston groove, thus reducing the possibility of micro-welding between the piston ring and the piston groove. The top compression ring usually has a parabolic or a barrel profile at its front face in order to enhance the hydrodynamic lubrication between the ring face and the cylinder wall interface (**Figure 9**).

The sealing capability of the top compression ring has significant influence of engine blowby because of the high gas pressure gradient across the top ring. Engine blowby is recognized as the high-pressure gas leaking into the crankcase through the ring pack. Thus, the top compression ring is desired to conform to the cylinder wall evenly along the ring circumference. Also, due to the high gas pressure gradient across the top ring, the top ring stays against the bottom side of the piston groove most of the time during the engine cycle.

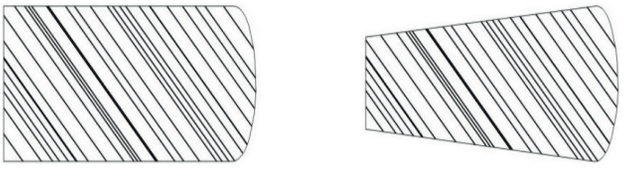

Figure 9. Top compression ring cross section.

1.2.2. Second compression ring

The second ring is a scraper ring which is recognized as 80% for scraping the lubrication oil down and 20% for sealing the combustion chamber. Because of the wedge effect, the scraper ring promotes hydrodynamic lubrication during the up-strokes (compression and exhaust strokes) and scrapes oil down during the down-strokes (intake and expansion strokes). **Figure 10** shows two types of second rings: one is scraper ring and the other is Napier ring. For the second ring, static twist is usually introduced by cutting off the ring material at one of the back corners. If the lower inside corner is cut off, the ring is a negative static twisted ring, while if the upper inside corner is cut off, the ring has a positive static twist configuration.

Although the gas pressure gradient across the second compression ring is much lower than that of the top ring, the second ring also has a noticeable effect on gas flow and gas dynamics. Due to this lower-pressure gradient across the second ring, the ring inertial force becomes competitive to gas pressure force. The inertial force may lift the second ring up at late compression stroke such that the second ring stays against the top flank of the groove. This process may repeat depending on the pressure buildup above the second ring when it is top seated. This unstable axial in-groove motion is recognized as ring fluttering [12]. When the ring fluttering occurs, another gas flow path between the ring and groove sides opens. As a result, blowby gas may increase.

It is also possible for the second ring to move inward in the radial direction. This radial movement is known as ring radial collapse [12]. When the ring radial collapse occurs, the gas above the ring can flow past the ring directly between the ring face and the cylinder wall to the lower land. Severe engine blowby can occur at this ring collapse condition. It depends on the ring and piston design which of the two conditions occur, ring fluttering or ring collapse. It is also possible that the two conditions occur simultaneously.

It was found that the static twist has significant influence on the second ring fluttering and radial collapse. The second ring with a negative static twist is more likely to flutter than a positive static twist second ring. However, if the second ring is lifted against the top flank of the groove, the positive static twist configuration will be more likely to collapse than the negative twist configuration. This will be discussed in the "Ring dynamics" section later in this chapter.

1.2.3. Oil control ring

The oil control ring is used to meter and distribute lubrication oil onto the cylinder wall. There are generally two types of oil control rings: two-piece oil control ring and three-piece oil

Figure 10. Second compression ring cross section.

control ring (**Figure 11**). The two-piece oil control ring consists of a ring body with two rails and a helical spring on the back providing the ring tension force. The three-piece oil control ring consists of two segments and an expander in between the two segments. The expander provides the radial force to conform the ring to the cylinder wall and also the axial force to push the ring against the top and bottom sides of the groove. The oil control ring is a two-direction scraper ring that scrapes oil in both upward strokes and downward strokes. During the downward strokes, the bottom rail/segment scrapes oil directly back into the crankcase. The top rail/segment scrapes oil back into the groove through the oil control ring expander. Generally, holes at the back of the oil control ring groove can be found along the circumference in order to allow the oil draining to the crankcase. In some piston design, instead of using these holes at the back of the groove, cast slots are introduced at the bottom edge of the groove for oil drain as an easier solution. During the upward strokes, the bottom rail/segment scrapes oil into the groove through the expander. The recovery of oil scraped by the top rail/segment during these upward strokes depends on the external force on the top rail/segment. At times, the external axial force on the oil control ring overcomes the expander force. As a result, an oil flow crevice is formed between the oil control ring and the groove sides allowing the oil drain into the groove and eventually back to the crankcase.

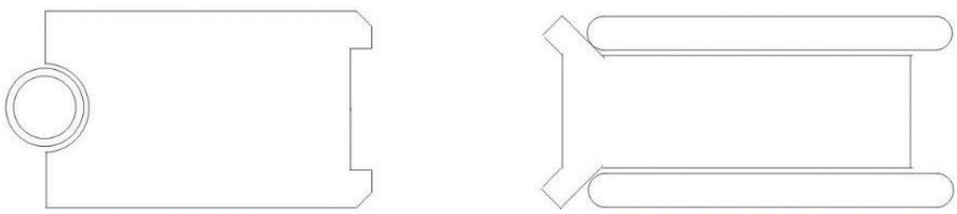

Figure 11. Oil control ring: two-piece oil control ring (left), three-piece oil control ring (right).

1.3. Cylinder

The cylinder of a reciprocating engine is the part through which the piston travels. The cylinder may be sleeved or sleeveless depending on the metal used for the engine block. For example, a cast iron engine block generally does not require cylinder sleeve because the iron is hard enough to resist wear between the piston ring and the cylinder wall. However, for aluminum alloy engine blocks that can be found in almost all daily drive cars, cylinder sleeves are required since the aluminum alloy is not hard enough to resist wear between the piston ring and the cylinder wall interface.

Cylinder liners, or cylinder sleeves, are manufactured nowadays using the centrifugal casting process. The centrifugal casting process refers to the technique for casting, which has a permanent mold spinning continuously along its center line at a constant speed. At the same time, molten metal is poured to the mold and thrown toward the inside wall of the mold. Then, the molten metal is solidified after cooling. The spinning orientation of the casting machine can be either horizontal or vertical, depending on the parts it is producing. Horizontal spin is preferred for long and thin cylinder, while vertical spin is preferred for short and wide cylinders. Aluminum engines without sleeves can also be found. The aluminum cylinders are

treated with nickel silicone alloy coating or other plasma coating that help reduce cylinder wear. Other techniques have also been explored by the researchers in order to reduce engine friction. One method is to introduce dimples at the mid-stroke to the cylinder walls [13]. This helps reduce friction because at the mid-stroke, the piston rings are generally under hydrodynamic friction when the piston speed is high. By introducing the dimples to the cylinder wall, the effective area of contact between the ring faces and the cylinder wall has been reduced. This leads to reduction of viscous friction as claimed.

Typical surface roughness for cylinder liner is 0.4–0.5. This roughness has been reduced significantly, which could help reduce engine oil consumption. Rougher cylinder walls can help retain lubrication oil on the liner surface between micro-valleys, which is similar to the dimple liner [13]. As a result, friction between the ring/cylinder wall and the piston skirt/cylinder wall interfaces can be reduced due to the lubrication oil in the micro-valleys. However, this micro-valley-retained oil is not scraped from the liner during engine down-strokes and can stay exposed to high-temperature gases. As a result, more oil is evaporated and the oil consumption increases.

Cylinder liners are no longer circular when the engine is in operation. The deformation results from mechanical distortion from bolting the cylinder block to the cylinder head, thermal distortion when the thermal load on the liner is not uniform, mechanical load when piston is slapping into the liner, the pressure load from the combustion event, and so on. Cylinder bore distortion is measured from an experiment by researchers [14]. For modeling concern, the cylinder bore distortion is usually defined by a Fourier series [4, 5]:

$$\delta R = \sum_{i=0}^{i=4} \left(A_i \cos(i\theta) + B_i \sin(i\theta) \right) \tag{1}$$

where δR is the deviation from roundness, A_i and B_i are Fourier coefficients and i is the order of the series.

The orders of the distortion are recognized in **Table 2**.

Zero order	Change in bore diameter
First order	Bore eccentricity
Second order	Oval deformation
Third order	Three-lobe deformation
Fourth order	Four-lobe deformation

Table 2. Cylinder bore distortion.

2. Ring pack dynamics

The piston ring dynamics is closely related to their functions, especially for gas control and oil control. Although the top ring is the most important part for gas sealing, while the oil

control ring has the highest effect in control oil flow and consumption, the second ring also has significant influence on both gas and oil control. This section discusses the ring dynamics of the second compression ring. The theories can also be applied on the top compression ring and oil control ring as well and the details of the ring dynamics models can be found from Refs. [15–20].

As discussed in Section 1, there are two types of ring dynamics: ring fluttering and ring radial collapse. Piston ring fluttering is the axial movement under the consequence of external force unbalance, especially between gas pressure force and inertial force. The other loads acting on the ring, including friction force, oil film squeezing force, and so on, are relatively small in comparison [6]. It is noted that while the second ring friction is relatively low, the friction forces of the oil ring and the top ring during high cylinder pressures can be large. Also, only the second ring flutter and collapse that occurs around top dead center (TDC) firing conditions is described here. This region is also considered the most important region for ring fluttering and collapse because of its significance on blowby and oil consumption.

Another phenomenon, radial collapse, can occur if the ring is lifted and seated against the top of the ring groove. When the ring is on the top side of the ring groove, the pressure force not only pushes the ring downward but also acts on the front face of the ring pushing it inward. The ring seals the gas pressure at the top, meaning the pressure behind the ring can be much lower. When the pressure force on the ring face exceeds the ring tension and the pressure force behind the ring, the ring collapse will occur. Once it collapses, the gases will escape past the ring face and equalize all around the rings. Once again, there will be no net gas pressure on the ring and the elastic tension of the ring will force the ring back out to the cylinder wall. As can be expected, there is no sealing between the ring face and the cylinder wall. As a result, the gas flow can pass the ring face resulting in high blowby. The ring collapse is one of the unstable behaviors of the ring.

It will depend on the ring and piston design as well as the operating conditions if ring flutter or collapse can occur. It is also possible that both ring flutter and collapse occur at the same time. In either case, the second ring loses its sealing capability allowing gases flowing either around the ring (in the fluttering case) or past the ring face (in the ring collapse case).

The ring design itself also has significant influence on its stability, for example, ring static twist. A negative-twisted second ring forms an outer edge seal between the ring and groove bottom sides when the ring is at the flank bottom. This allows gases to flow underneath the ring resulting in a very low net downward gas pressure force. In this case, the ring can be easily lifted by the inertial force acting on the ring (**Figure 12a**). On the other hand, for a positive static twisted second ring, the seal between the ring and the groove bottom occurs at the inner bottom corner. This prevents higher-pressure gas moving between the ring bottom and the groove bottom, resulting in a higher downward pressure force. The ring is not easy to be lifted by inertial force. **Figure 12a** depicts a simplistic illustration showing the gas pressure forces acting on the sides of the rings.

Similarly, the ring top-seating stability (**Figure 12b**) can be explained similarly as for the bottom-seating condition. However, it should be noted that since a negative-twisted ring is easier

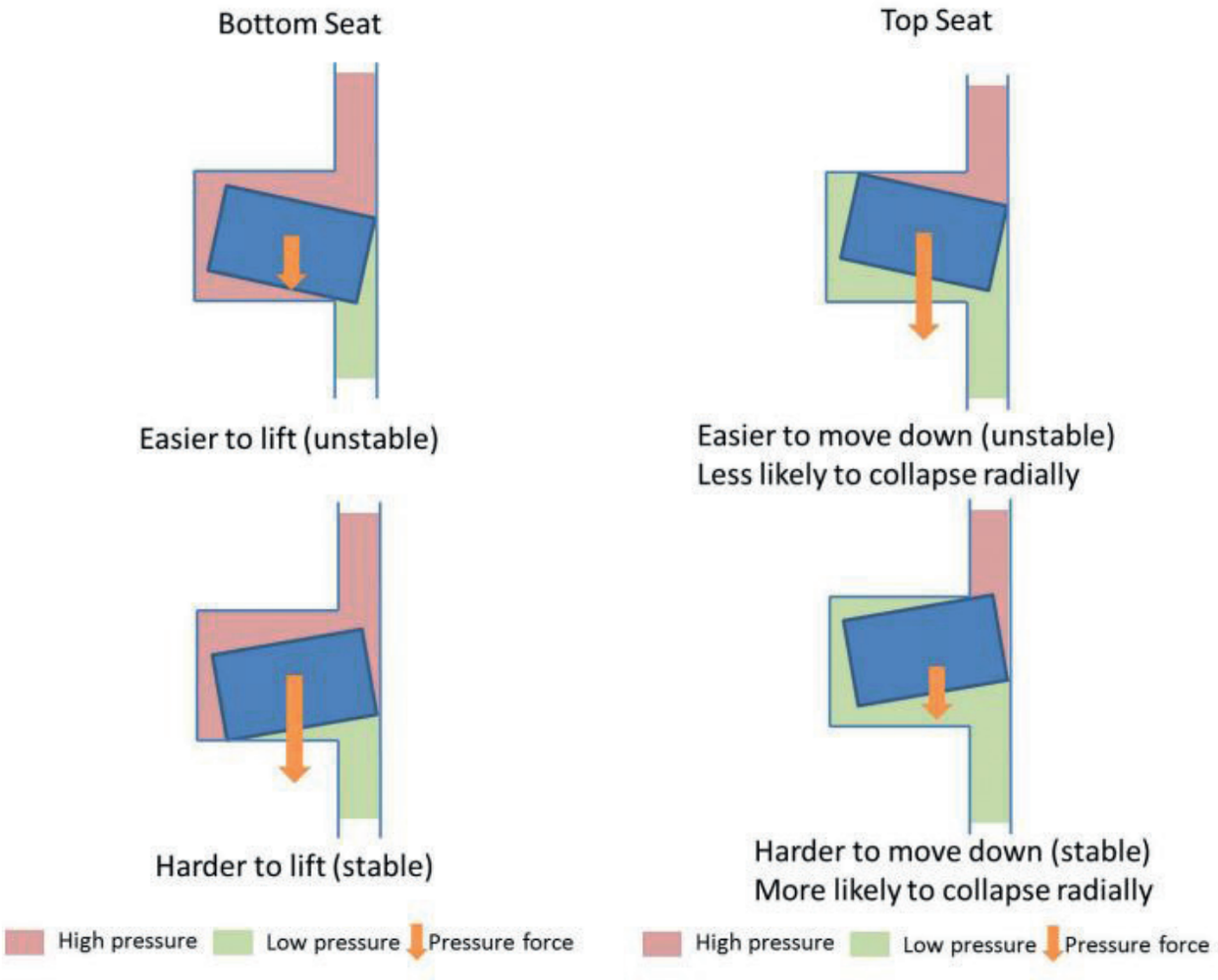

Figure 12. Ring-seating stability: (a) bottom-seating stability and (b) top-seating stability.

to move down, it will be less likely to collapse. Conversely, the positive-twisted ring will be more difficult to push down; therefore, the ring will be more likely to collapse radially inward as the pressure above the ring can become higher. In summary, the configuration with positive static twist tends to increase the pressure force holding the second ring down and promoting second ring stability. This positive twist ring is also more susceptible to collapse. On the contrary, the configuration with a negative static twist will tend to promote ring flutter. However, ring radial collapse is less susceptible to occur.

When the second ring flutters or collapses, the blowby will generally be higher. This is because the ring does not seal the gases and the gases flow past the ring. While this can cause high blowby, the pressure in the second land will be very low. This will prevent reverse blowby, which is beneficial for oil consumption. More discussions about ring pack dynamics can be found from Refs [17–20].

Nowadays, researchers from the industry and the academic area are developing the ring pack dynamics model in three-dimensional (3D) in order to capture the variation along the ring

circumference with the consideration of cylinder liner ID deformation. In addition, the influence from piston secondary motion can also be implemented to further understand the ring pack behavior. This will capture the gas flow in the circumference direction, which the current commercial two-dimensional (2D) models are not capable of. As a result, the ring dynamics, oil consumption, friction, and wear for the ring pack can be better modeled and understood to guide design. The next section is an introduction to the 3D modeling work for the ring pack.

The 2D ring pack dynamics model is still widely used in the automotive and heavy-duty industries during product development, given the experience and fidelity built on this approach. Some improving activities include implementing wear model at the ring face and side based on different wear mechanism, oil consumption model due to oil evaporation, oil throw-off, oil scraped back to the combustion, and so on. In addition, 3D ring pack dynamics models are being developed using different approaches, including full FEA with hexahedron element, discretizing the ring using space beam elements, and so on, with different orders of success. The 3D model approach will be discussed in the next section with more detail.

3. Ring-piston groove-cylinder liner interaction

In engine power cylinder system development, utilizing CAE tool has become a standard approach to design and optimize the system. Traditional CAE tools are two-dimensional (2D) which considers the ring motion along the cylinder axis and the twist. However, the variation along the ring circumference is assumed to be identical. The demand for better understanding of the power cylinder system requires three-dimensional (3D) CAE tools to simulate the variation along the ring circumference as well. Researchers have started working on 3D modeling. One variation along the ring circumference is the contact pressure between the ring face and the cylinder bore interface, and the ring side and piston groove side interface. The interactions are discussed in this section.

3.1. Ring-cylinder bore contact

When the free-state ring is installed into the cylinder liner, the ring is constrained at its front face by the cylinder wall. Every point on the ring front face needs to be tracked whether it is in contact with the cylinder wall or not. However, due to the computation time and resource, it is not possible with the existing computation tool. And the most important thing is how the contact force/pressure distributes along the ring circumference. Thus, in this section, the ring is specified constrained at 13 different cross-section locations along the circumference [21–23]. The ring conformability is modeled using finite element method (FEM) [24, 25] for a keystone compression ring. The approach solving the problem is based on penalty method-based optimization that minimizes the strain energy of the piston ring [26–30].

As shown in **Figure 13**, the middle constraint locates at the ring back (opposite to the ring gap) front face. Other constraints are symmetric about the ring back and distribute with an increment of about 30°. The free-shape ring mesh and the deformed ring mesh without temperature compensation are shown in **Figure 13**.

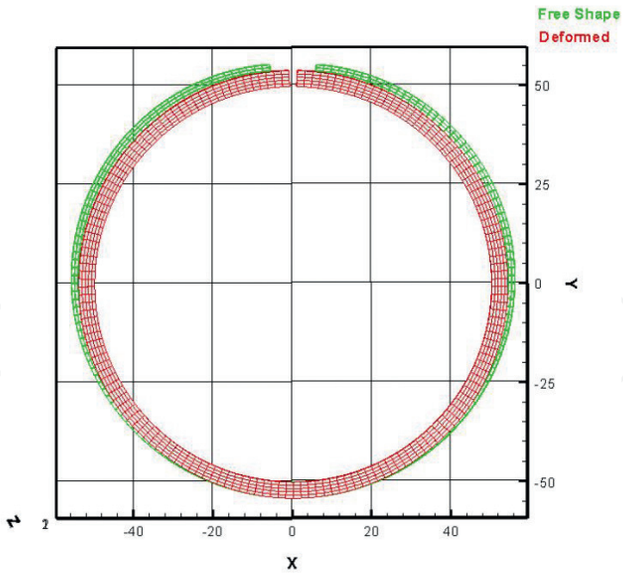

Figure 13. Free-shape and deformed ring meshes.

The green mesh shown in **Figure 13** represents the free-shape ring while the red mesh represents the deformed ring shape under the cylinder bore constraints without temperature compensation. It is obvious that the ring is pushed inward from its free state. The constraint forces that push the ring to its deformed position are shown in **Figure 14**. The blue and red bars represent the constraint forces at a certain circumference location at the upper and lower corners at ring face. And the green and purple dots show the separation gaps between the ring face and the cylinder bore.

From **Figure 14**, it is found that the two contact forces at the same cross section are identical since the ring has a symmetric cross section and there is no twisting moment on the ring. The

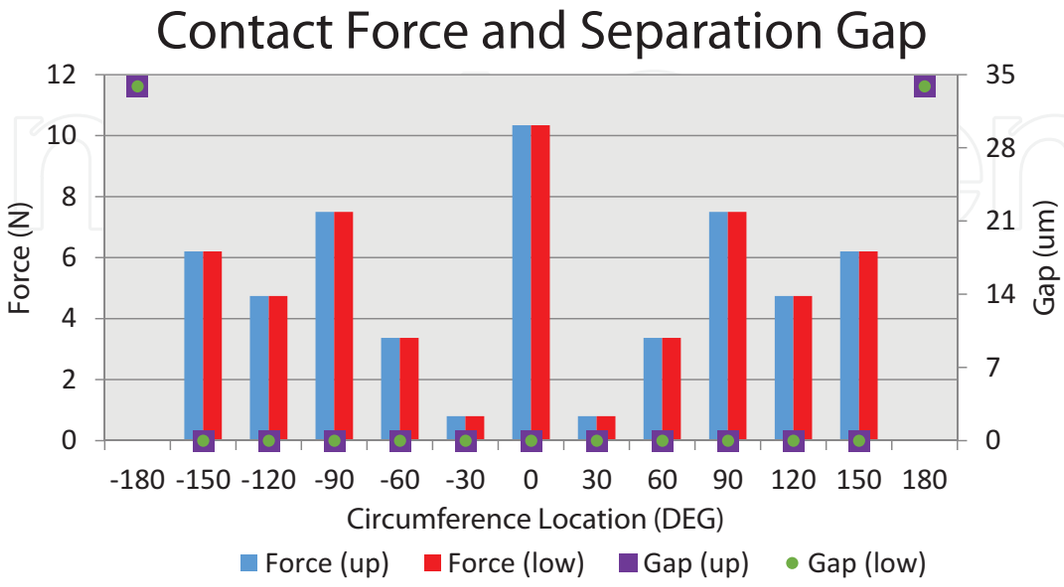

Figure 14. Constraint force and separation gap.

plot also shows that the constraint force at the ring back is the highest. At the cross sections approximately 30° away from the ring back, the lowest constraint forces are found for the sections that are in contact against the cylinder wall. The constraint forces at the ring tips vanish such that the ring separates from the cylinder wall in its front face at its two tips. The separation gap is defined as the radial distance between the cylinder wall ID and the ring tip OD. A 34-μm separation gap is found for this specific ring from the FEA model.

3.2. Result of ring-cylinder bore-groove side contact

Another example is given in this section for ring-cylinder bore-groove side contact using a scraper ring with a positive static twist. The scraper ring has a taper face and cuts off at the ring inner upper corner, which promotes positive twist when installing the ring into the piston groove. The cross section of the scraper ring is shown in **Figure 15**.

From **Figure 15**, four nodes of the cross section at a given circumference location are considered for the ring-piston groove side interaction and are numbered as node 1, node 2, node 3, and node 4 as shown. These four nodes are constrained by the groove in the axial direction. This means nodes 1 and 2 should stay in contact or above the groove bottom side, while nodes 3 and 4 should stay in contact or below the groove top side. Two nodes on the ring front face are constrained by the cylinder bore in the radial direction, at the front face top and bottom edges, respectively. The groove has zero angles at its top and bottom sides. The nominal clearance between the groove and the ring axial thicknesses is 0.1 mm.

The main parameters describing the ring are listed in **Table 3**.

The constraint locations along the ring circumference are equally spaced with about 30° from one butt end to the other. The number of constraint locations is found to be able to represent the ring/cylinder liner/groove side contact force/pressure distribution pattern and also save calculation time. Increasing constraint locations will increase computation time exponentially, while decreasing the constraint locations may result in the contact force/pressure pattern not being able to be well represented.

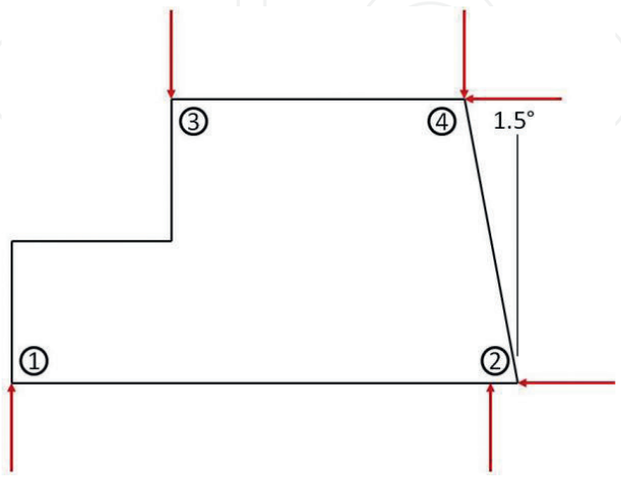

Figure 15. Constraints on ring cross section.

Ring material	Steel
Modulus of elasticity	200.0 GPa
Poisson's ratio	0.3
Cylinder bore diameter	108.0 mm
Coefficient of thermal expansion	13.0E-6/°C
Thermal conductivity	45 W/m K
Ring/gas-convective coefficient	25 W/m^2 K
Ring/oil film-convective coefficient	100 W/m^2 K

Table 3. Main parameters for the ring.

The deformed ring shape is shown in **Figure 16** after installing into the cylinder liner and piston groove. The displacement in the *z*-direction (axial direction) is amplified by 100 times in order to illustrate the ring deformation distinctly.

In this case, the ring back and ring butt ends are in contact with the groove bottom side, while the ring touches the groove top side at about 60° from the end gap (120° from the ring back). The constraint forces between the ring and the piston groove sides are important since it dictates the contact pattern which will affect the ring-groove side wear eventually. More details about the ring, cylinder liner, and piston groove interactions can be found from Refs. [22, 23].

Ultimately, the interactions between the ring face-liner bore interface and the ring side-piston groove side interface are used to model the wear between them [17] as well as the ring pack dynamics that heavily influences engine oil consumption, to further optimize the ring pack and power cylinder design and improve the durability of the subsystem.

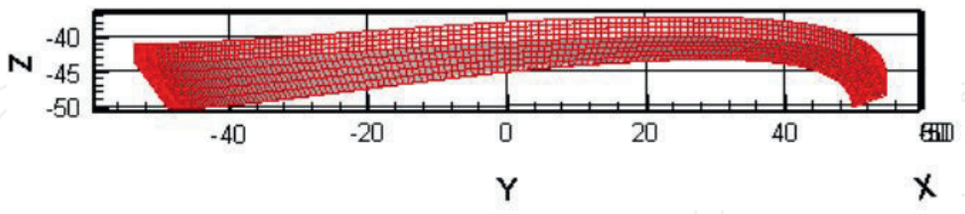

Figure 16. Deformed ring shape after installing into the cylinder liner and piston groove.

Author details

Chao Cheng

Address all correspondence to: chengc22@msu.edu

Michigan State University, MI, USA

References

[1] Richardson DE. Review of power cylinder friction for diesel engines. Journal of Engineering for Gas Turbines and Power. 2000;**122**(4):506-519

[2] Heywood JB. Internal Combustion Engine Fundamentals. New York, NY: McGraw-Hill; 1988

[3] Patel P, Mourelatos Z, Shah P. A comprehensive method for piston secondary dynamics and piston-bore contact. In: SAE World Congress; Detroit, MI. 2007. 2007-01-1249

[4] Keribar R, Dursunkaya Z, Ryan J. A Comprehensive Model of Piston Skirt Lubrication. SAE Technical Paper 920483, International Congress & Exposition, Detroit, Michigan; February 24-28, 1992

[5] Wong V, Tian T, Lang H, Ryan J, Sekiya Y, Kobayashi Y, Aoyama S. A Numerical Model of Piston Secondary Motion and Piston Slap in Partially Flooded Elastohydrodynamic Skirt Lubrication. SAE Technical Paper 940696, International Congress & Exposition, Detroit, Michigan, February 28 - March 3, 1994

[6] Cheng C, Akinola A. Piston friction reduction by reducing piston compression height for large bore engine application. In: SAE World Congress, Detroit, MI. 2017. SAE 2017-01-1044

[7] Kim K, Godward T, Takiguchi M, Aoki S. Part 2: The Effects of Lubricating Oil Film Thickness Distribution on Gasoline Engine Piston Friction. SAE Technical Paper 2007-01-1247

[8] Kim K, Shah P, Takiguchi M, Aoki S. Part 3: A Study of Friction and Lubrication Behavior for Gasoline Piston Skirt Profile Concepts. SAE Technical Paper 2009-01-0193

[9] Westerfiled Z, Totaro P, Kim D, Tian T. An Experimental Study of Piston Skirt Roughness and Profiles on Piston Friction Using the Floating Liner Engine. SAE Technical Paper 2016-01-1043, SAE World Congress and Exhibition, Detroit, Michigan, Apail 12-14, 2016

[10] Kobayashi T. Prediction of Piston Skirt Scuffing via 3D Piston Motion Simulation. SAE Technical Paper 2016-01-1044, SAE World Congress and Exhibition, Detroit, Michigan, April 12-14, 2016

[11] Maurizi M, Hrdina D. New MAHLE Steel Piston and Pin Coating System for Reduced TCO of CV Engines. SAE Int. J. Commer. Veh. 2016;**9**(2):270-275.

[12] Cheng C, Schock H, Richardson D. The Dynamics of Second Ring Flutter and Collapse in Modern Diesel Engines. ASME J. Eng. Gas Turbines Power. 2015;**137**(11):111504-111504-8

[13] Urabe M, Takakura T, Metoki S, Yanagisawa, M, et al. Mechanism of and Fuel Efficiency Improvement by Dimple Texturing on Liner Surface for Reduction of Friction between Piston Rings and Cylinder Bore. SAE Technical Paper 2014-01-1661, SAE World Congress and Exhibition, Detroit, Michigan, Detroit, Michigan, April 8-10, 2014

[14] Bird L, Gartside R. Measurement of Bore Distortion in a Firing Engine. SAE Technical Paper 2002-01-0485, SAE 2002 World Congress, Detroit, Michigan, March 4-7, 2002

[15] Tian T, Rabute R, Wong V, Heywood J. Effects of Piston-Ring Dynamics on Ring/Groove Wear and Oil Consumption in a Diesel Engine. SAE Technical Paper 970835, SAE International Congress & Exposition, Detroit, Michigan, February 24-27, 1997

[16] Akalin O, Newaz GM. Piston ring-cylinder bore friction modeling in mixed lubrication regime: Part I—analytical results. Journal of Tribology. 1999;**123**(1):211-218

[17] Baker C, Rahmani R, Karagiannis I, Theodossiades S, Rahnejat H, Frendt A. Effect of Compression Ring Elastodynamics Behaviour upon Blowby and Power Loss. SAE Technical Paper 2014-01-1669. 2014

[18] Poort M, Cheng C, Richardson D, Schock H. Piston Ring and Groove Side Wear Analysis for Diesel Engines. ASME J. Eng. Gas Turbines Power. 2015;**137**(11):111503-111503-9

[19] Westerfield Z, Liu Y, Kim D, Tian T. A Study of the Friction of Oil Control Rings Using the Floating Liner Engine. SAE Int. J. Engines. 2016;**9**(3):1807-1824

[20] Ejakov M, Schock H, Brombolich L, Carlstrom C, Williams R. Simulation analysis of inter-ring gas pressure and ring dynamics and their effect on blowby. ICE-Vol. 29.2, ASME 1997 Fall Technical Conference

[21] Tomanik E. Improved Criterion for Ring Conformability Under Realistic Bore Deformation. SAE Technical Paper 2009-01-0190, SAE World Congress, Detroit, Michigan, April 20-23, 2009

[22] Cheng C, Kharazmi A, Schock H, Wineland R, Brombolich L. Three-Dimensional Piston Ring-Cylinder Bore Contact Modeling. ASME J. Eng. Gas Turbines Power. 2015;**137**(11): 111505-111505-10

[23] Cheng C, Kharazmi A, Schock H. Modeling of piston ring-cylinder bore-piston groove contact. In: SAE World Congress; Detroit, MI, 2015. SAE 2015-01-1724

[24] Fish J, Belytschko T. A First Course in Finite Elements. Chichester, England; Hoboken, NJ: John Wiley & Sons Ltd.; 2007. pp. xiv, 319 p., 318 p. of plates

[25] Cook RD. Finite Element Modeling for Stress Analysis. John Wiley & Sons, Inc.; 1994

[26] Song X, Diaz AR, Benard A, Nicholas JD. A 2D model for shape optimization of solid oxide fuel cell cathodes. Structural and Multidisciplinary Optimization. 2012;**47**:453-464

[27] Song X, Diaz AR, Benard A. A 3D topology optimization model of the cathode air supply channel in planar solid oxide fuel cell. In: Proceedings of the 10th World Congress on Structural and Multidisciplinary Optimization; May 19-24; Orlando, FL, USA. 2013

[28] Panayi AP, Diaz AR, Schock HJ. On the optimization of piston skirt profile using a pseudo-adaptive response surface method. Structural and Multidisciplinary Optimization. 2009;**38**:317

[29] Yu J, Dong X, Wang W. Prototype and test of a novel rotary magnetorheological damper based on helical flow. Smart Materials and Structures. IOP Publishing Ltd.; 2016;**25**(2).

[30] Dong X, Yu J, Yang M. Optimization and experimental study of magneto-rheological fluid damper considering temperature effects. Journal of Vibration and Shock. 2016;**35**(8)

IntechOpen